Plant Physiol. (1988) 87, 491–497
0032-0889/88/87/0491/07/$01.00/0

Preparation of Corn Root Plasmalemma with Low Mg-ATPase Latency and High Electrogenic H^+ Pumping Activity after Phase Partitioning[1]

Received for publication November 3, 1987 and in revised form February 26, 1988

NATHALIE GALTIER, ANDRES BELVER[2], RÉMY GIBRAT, JEAN-PIERRE GROUZIS, JACQUELINE RIGAUD, AND CLAUDE GRIGNON*
Biochimie et Physiologie Végétales, Institut National de la Recherche Agronomique, Centre National de la Recherche Scientifique (UA 573), Ecole Nationale Supérieure Agronomique, 34060 Montpellier Cedex, France

ABSTRACT

Crude plasma membranes of corn (*Zea mays* L.) roots were obtained according to MI De Michelis and RM Spanswick (1986 Plant Physiol 81: 542–547). This preparation, which contained tightly sealed vesicles displaying Mg-ATP dependent H^+-transport, was purified by phase partitioning. The percentage of inside-out vesicles (10%) was determined from the Mg-ATPase latency, revealed with lysophosphatidylcholine. A Triton X-100 treatment described previously (JP Grouzis, R Gibrat, J Rigaud, C Grignon 1987 Biochim Biophys Acta 903: 449–464) was applied to phase-partitioned plasma membranes. The percentage of catalytic sites freely accessible to Mg-ATP increased to 50% after Triton X-100 treatment. Treated vesicles remained capable of electrogenic H^+-pumping, as demonstrated by Mg:ATP-dependent quinacrine fluorescence quenching and oxonol absorbance shift. As expected from the large increase of the catalytic sites accessibility, increases of the dye responses were observed. Concanavalin A binding was estimated from microelectrophoretic measurements of individual vesicles. Statistical analysis of concanavalin A binding and Mg-ATPase latency suggest that treated membranes have lost their asymmetric structure.

The plant plasma membrane contains a vanadate-sensitive Mg-ATPase which operates in the electrogenic extrusion of H^+ (26). It has been well demonstrated that plasma membrane preparations from various plant tissues isolated by phase partitioning are highly purified (18). Unfortunately, these preparations consist mainly of sealed right-side out vesicles, where the H^+-ATPase catalytic sites are inaccessible to Mg-ATP (17). Furthermore, active H^+-transport by inside-out plasmalemma vesicles of cereals is particularly difficult to study, most likely due to leakiness of the membrane (27) following purification by sucrose gradient centrifugation or by phase partitioning (6). Recently, a differential centrifugation method has been described to obtain tightly sealed plasmalemma vesicles from corn roots, exhibiting Mg:ATP-dependent H^+-transport (9). In a previous paper (13), we have shown that the crude plasmalemma fraction isolated according to this method contained only approximately 30% inside-out vesicles. We have also described a method, using Triton X-100 treatment, to increase this proportion up to 65%, while maintaining the tightness of the vesicles to H^+ (13). Similar Triton X-100 treatment of phase-partitioned plasmalemma has been previously reported (7). In this paper, we have further investigated the effect of Triton X-100 treatment on Mg-ATPase latency, vesicle sidedness, H^+-transport, and membrane potential of corn root plasma membrane purified by phase partitioning. After Triton X-100 treatment, all the vesicles bound Con A while half of the Mg-ATPase catalytic sites remained freely accessible to Mg-ATP. These data are consistent with the assumption of the loss of membrane asymmetric structure.

MATERIALS AND METHODS

Preparation of Microsomal Vesicles. Microsomes were prepared according to De Michelis and Spanswick (9). Briefly, 5 d old corn (*Zea mays* L.) roots were gently chopped with razor blades and ground with mortar and pestle in 4 ml per g fresh weight of grinding medium containing 0.5% BSA, 25 mM BTP[3]-Cl (pH 7.6), 250 mM sucrose, 2 mM DTT, 2 mM $MgSO_4$, 2 mM ATP, 10% glycerol, 2 mM EGTA, and 1 mM PMSF. The homogenate was filtered and centrifuged for 10 min at 13,000*g*. Crude microsomes in the resulting supernatant were pelleted for 30 min at 80,000*g*. To obtain KI-washed microsomes, crude microsomes were resuspended in grinding medium containing 250 mM KI, incubated on ice for 15 min, and then sedimented for 30 min at 80,000*g*. Crude and KI-washed microsomes were finally resuspended in a medium containing 0.2% BSA, 2 mM BTP-Cl (pH 7.0), 250 mM sucrose, 10% glycerol, 1 mM DTT, and were stored in liquid N_2.

Phase Partition. Crude or KI-washed microsomes were purified using a two-phase system composed of 6% (w/w) Dextran T500, 6% (w/w) polyethylene glycol 3350, 250 mM sucrose, 10 mM K^+-phosphate (pH 7.8), 1 mM ATP, 1 mM EDTA, and 30 mM NaCl at 0°C. One mg of membrane protein was added to 8 g phase system and vigorously mixed by shaking. The phase settling was facilitated by centrifugation for 5 min at 4,000*g* in a swinging bucket centrifuge. The purified plasma membranes were collected in the upper phase, diluted five-fold in 2 mM BTP-Cl (pH 7.0) containing 250 mM sucrose and 1 mM DTT, and then pelleted for 35 min at 80,000*g*. Pellets were resuspended in resuspension medium and stored in liquid N_2.

[1] Supported by Ministère de la Recherche et de l'Industrie (Action Concertée 84C 1406) and a Centre National de la Recherche Scientifique graduate fellowship to A.B.

[2] Present address: Estacion Experimental del Zaidin, Bioquimica vegetal, 18008 Granada, Spain.

[3] Abbreviations: BTP, 1,3-bis(tris(hydroxymethyl)amino)propane; lysoPC, lysophosphatidylcholine; PMSF, phenylmethylsulphonylfluoride.

Triton X-100 Treatment. The medium used is the resuspension medium. Purified plasma membranes were incubated with stirring for 10 min at 0°C in the presence of various Triton X-100 concentrations. Thereafter, they were sedimented for 35 min at 80,000*g*, resuspended to eliminate Triton X-100, and sedimented again. Finally, pellets were resuspended in resuspension medium and stored in liquid N_2.

Enzymic Marker Assays. Nucleoside phosphate hydrolysis was assayed in a 0.5 ml reaction volume as indicated below. Reactions were started by addition of 1 to 10 μg protein, incubated for 30 min at 26°C, unless otherwise indicated. Reactions were stopped, and Pi was assayed, by addition of 1 ml Ames reagent (1) containing 0.1% SDS (w/v).

The plasma membrane Mg-ATPase activity was operationally defined as the vanadate-sensitive, molybdate-insensitive Mg-ATP hydrolysis (10). The assay medium contained 50 mM BTP-Cl (pH 6.5), 100 mM KCl, 5 mM BTP-ATP, 5 mM $MgSO_4$, and 0.1 mM Na-molybdate with or without 0.25 mM orthovanadate. The basal activity (*i.e.* the activity of inside-out vesicles) is the activity measured in the presence of 10 mM NH_4Cl and in the absence of the permeabilizing agent lysoPC. Ammonium chloride was added to dissipate the pH gradient, in order to obtain maximal Mg-ATPase activity. Reversion of quinacrine quenching (not shown) indicated that 10 mM NH_4Cl was effective in dissipating the pH gradient. The Mg-ATPase activity of both inside-out and right-side-out vesicles is measured in the presence of 10 mM NH_4Cl plus 0.1 mM lysoPC (13). The latent activity (*i.e.* the activity of right-side-out vesicles) is the difference between the activities measured with and without lysoPC. The latency is the latent activity expressed as a percentage of the activity in the presence of lysoPC.

Golgi concentration was estimated by latent IDPase according to Green (12), except that the latency was tested by addition of lysoPC rather than by storage for 3 d at 4°C. The assay medium contained 50 mM BTP-Cl (pH 7.2), 100 mM KCl, 5 mM Na-IDP, 5 mM $MgSO_4$, and 0.1 mM Na-molybdate. Latent IDPase is the difference between the activities measured in the presence and in the absence of 0.1 mM lysoPC

Mitochondrial contamination was estimated by azide-sensitive Mg-ATPase. The assay medium contained 50 mM BTP-Cl (pH 8.5), 100 mM KCl, 5 mM BTP-ATP, 5 mM $MgSO_4$, 0.1 mM Na-molybdate, and 0.1 mM lysoPC with or without 1 mM NaN_3.

Tonoplastic contamination was estimated by NO_3^--sensitive Mg-ATPase. The assay medium contained 50 mM BTP-Cl (pH 8.5), 5 mM BTP-ATP, 5 mM $MgSO_4$, 0.1 mM Na-molybdate, 0.1 mM lysoPC, and 100 mM KCl or KNO_3. Nitrate-sensitive Mg-ATPase is the difference between the activities measured in the presence of KCl and KNO_3 (21).

Proton Transport Assays. The specific initial rate of fluorescence quenching of quinacrine was used to monitor the initial H^+-pumping activity (5). The assay medium (2 ml) contained 50 mM BTP-Cl (pH 6.5), 100 mM KCl or KNO_3, 5 mM BTP-ATP, 0.1 μM valinomycin, 10 μM quinacrine, and 40 to 400 μg membrane protein. After incubation for 20 min at 26°C, the reaction was started by addition of 5 mM $MgSO_4$. Fluorescence was recorded at excitation/emission wavelengths of 423/500 nm with a Jobin-Yvon JY3-CS apparatus. The initial rate of quenching was linear with protein concentration (at least up to 200 $\mu g \cdot ml^{-1}$) and thus can be expressed in specific units (% quenching$\cdot min^{-1} \cdot mg^{-1}$ protein).

Membrane Potential Detection. The anionic probe oxonol VI was used for monitoring the membrane potential, positive inside, generated by the electrogenic H^+-pumping. This induced a shift of the absorption spectrum, due to an additional binding of the permeant dye on the inner layer of membrane, following its potential-dependent accumulation inside the vesicles (3). The amplitude of the shift depends on (a) the binding of oxonol to membranes and the concentrations of membranes and oxonol and (b) the membrane potential of these vesicles. Dye response depends also on the percentage of active vesicles (tightly sealed inside-out vesicles, *i.e.* impermeable to small ions, and sustaining an ATPase capable of electrogenic H^+-pumping) (27). The maximum amplitude of the absorbance shift and the isosbestic point were observed at 622 and 602 nm, respectively. Absorbance was time-recorded at 622 nm (A_{622_t}) and 602 nm (A_{602_t}) with a diode array spectrophotometer Hewlett-Packard HP 8451A and was numerically stored. To avoid interactions of oxonol with BSA, membranes were washed in BSA-free resuspension medium. The assay medium (2 ml) contained 50 mM BTP-SO_4 (pH 6.5), 50 mM K_2SO_4 or indicated salts, 5 mM BTP-ATP, 80 to 200 μg membrane protein, and 4 μM oxonol. The absorbance of the membrane suspension (due to turbidity) was measured at 602 and 622 nm before oxonol addition and is noted as D_{602} and D_{622}, respectively. After incubation for 20 min at 26°C, the total (bound plus free) and bound oxonol concentrations were determined according to Bashford *et al.* (4) and designated Ox_T and Ox_b, respectively:

$$Ox_T = (A_{602_{t=0}} - D_{602})/\epsilon_{f602} \quad (1)$$

$$Ox_b = (A_{622_{t=0}} - D_{622})/(\epsilon_{b622} - \epsilon_{f622}) \quad (2)$$

where ϵ_{f602}, ϵ_{f622}, and ϵ_{b622} are the molar absorbance coefficients of, respectively, free oxonol at 602 and 622 nm, and bound oxonol at 622 nm (ϵ_{f602} = 85 L $\cdot$ mmol^{-1}, ϵ_{f622} = 21 L $\cdot$ mmol^{-1}, and ϵ_{b622} = 105 L $\cdot$ mmol^{-1}). The reaction was started by addition of 5 mM $MgSO_4$. Traces presented are the absorbance at 622 nm corrected for dilution due to successive additions as follows, and noted (A'_{622_t}):

$$A'_{622_t} = A_{622_t} \times A_{602_{t=0}}/A_{602_t} \quad (3)$$

The increment of bound oxonol (ΔOx_b) after membrane energization was calculated as follows:

$$\Delta Ox_b = (A'_{622_t} - A_{622_{t=0}})/(\epsilon_{b622} - \epsilon_{f622}) \quad (4)$$

Microelectrophoretic Measurements. A Rank Brothers Mark II apparatus fitted out with an ultrathin-walled cylindrical glass cell (2) and an ultramicroscope illumination device was used for measuring the microelectrophoretic mobility of single vesicles. Very small particles (*e.g.* single plasmalemma vesicles) could be detected as brilliant points against a dark field. The medium (25°C) contained 25 mM Tris adjusted to pH 6.5 with Mes (Tris is a univalent cation at this pH), 10 μM $CaCl_2$, 10 μM $MnCl_2$, and Con A when indicated. The zeta potential was calculated from the mean microelectrophoretic mobility of 50 vesicles, unless otherwise indicated, with the help of the Helmholtz-Smoluchowski relation (15). The classical Gouy-Chapman relation was used to calculate the electrostatic charge density from the zeta potential (11, 20). The electrostatic surface charge of 150 or 300 vesicles was determined in order to study the distribution of this parameter. The Ross's Maximal Likelihood Program, distributed by the Statistics Department of Rothamsted Experimental Station (Herts, U.K.), was used for statistical analysis (24).

Other Methods. The results are given as means of four or more independent repetitions, and the confidence limits are 95%. Proteins are determined according to Schaffner and Weissman (25).

Chemicals. The sources of the compound studied were as follows: lysophosphatidylcholine: Sigma; oxonol VI: Molecular Probes; polyethylene glycol: Union Carbide; Dextran T500: Pharmacia. All other chemicals were analytical grade.

RESULTS

Distribution of Membrane Markers after KI Washing and Phase Partitioning. Table I shows the distribution of various membrane

Table I. *Enzymic Markers and Protein Distributions at Successive Purification Steps*

Assays were performed at 26°C, unless otherwise indicated. Specific activities are given as μmol · mg^{-1} protein · min^{-1}. Vanadate inhibition is given as % inhibition for 0.25 mM vanadate at 26°C. Protein is given as mg per 100 fresh weight.

	Microsomes	KI-Washed Microsomes	Phase Partition-Purified Plasmalemma	Triton X-100-Treated Plasmalemma
Vanadate-sensitive Mg-ATPase[a]				
At 26°C	0.33	0.39 ± 0.07	0.99 ± 0.16	2.0 ± 0.3
At 30°C	0.43	0.59	1.57	3.0
At 38°C	0.85	1.04	2.40	4.6
Vanadate inhibition[a]	70	79	90	93
Latent IDPase	0.20	0.22 ± 0.05	0.07 ± 0.03	0.01
NO_3^--sensitive Mg-ATPase[a]	0.18	0.11 ± 0.03	0.04 ± 0.02	ND[b]
N_3^--sensitive Mg-ATPase[a]	0.17	0.12 ± 0.07	Undetectable	ND
Protein	30	21	2.85	0.98

[a] Assayed in the presence of 0.1 mM lysoPC. [b] Not determined.

markers, assayed in the presence of lysoPC, after KI washing and phase partitioning. Potassium iodide washing resulted in an increase (approximately 25%) of the plasmalemma Mg-ATPase activity. Potassium iodide washing caused, respectively, a 38 and a 29% decrease of the tonoplastic and mitochondrial Mg-ATPase activities, while latent IDPase was not significantly affected. Phase partitioning of KI-washed microsomes led to a high degree of plasmalemma purification, as indicated (a) by the 2.5-fold increase of the plasmalemma Mg-ATPase and (b) by the strong reduction of the tonoplastic Mg-ATPase (64% decrease), the latent IDPase (68% decrease), and the quasi-elimination of the mitochondrial Mg-ATPase. The inhibition of Mg-ATP hydrolysis by 0.25 mM vanadate increased after KI washing and phase partitioning, indicating an elimination of nonplasmalemma Mg-ATPases.

Triton X-100 Treatment of Phase Partitioned Plasmalemma. The Mg-ATPase latency was determined after Triton X-100 treatment of phase-partitioned plasmalemma at various Triton X-100/protein ratios and Triton X-100 concentrations. Thereafter, Triton X-100 was eliminated by washing in the presence of BSA, as described in "Materials and Methods." The latency decreased from 87% to 43% after Triton X-100 treatment, whatever the ratio of detergent/protein (R) between 1 and 4 (w/w) for 0.075% (w/w) Triton X-100 (Fig. 1A). The latency decreased to 50% by varying the detergent concentration between 0.05 and 0.1% for $R = 2$ (Fig. 1B). The Triton X-100/protein ratio and Triton X-100 concentration used in further experiments were 2 (w/w) and 0.075% (w/w), respectively. After this treatment, approximately 66% of the membrane protein was lost. Nevertheless, 80% of the total plasmalemma Mg-ATPase (*i.e.* the specific activity assayed in the presence of lysoPC × protein amount) was recovered after Triton X-100 treatment. Consequently, the Mg-ATPase activity of phase partitioned plasmalemma, in the presence of lysoPC, increased two-fold after Triton X-100 treatment, while the latent IDPase and the tonoplastic Mg-ATPase were completely eliminated (Table I). Finally, 20% of the total initial microsomal Mg-ATPase activity were recovered.

Mg-ATPase Hydrolysis, Latency, and H^+-Pumping at Successive Steps of Plasmalemma Purification. The basal Mg-ATPase activity (*i.e.* assayed in the absence of lysoPC), its latency, and the specific initial rate of quinacrine quenching were measured in parallel runs at successive purification steps. The basal activity did not increase (Table II) after KI washing and phase partition, in spite of the three-fold enrichment in plasmalemma Mg-ATPase (Table I). Subsequent Triton X-100 treatment induced a nine-fold increase of the basal activity (Table II). The ATPase latency of crude microsomes (69%) slightly increased after KI washing (75%), increased further after phase partition (89%), and strongly decreased after Triton X-100 treatment (51%). The kinetics of quinacrine quenching after energization of similar protein amounts of KI-washed microsomes, phase-partitioned, and of Triton X-100-treated plasmalemma vesicles, are shown in Figure 2. The specific initial rate of quenching, measured in the presence of 100 mM KNO_3, was not significantly modified after KI washing and phase partitioning (Table II). The important feature is the eight-fold increase of the initial H^+-transport after Triton X-100 treatment. Triton X-100 treatment increased the stimulation of the basal Mg-ATPase activity (data not shown) by 10 mM NH_4Cl from 7% (untreated vesicles) to 20% (treated vesicles), probably by improving membrane tightness to H^+ (13).

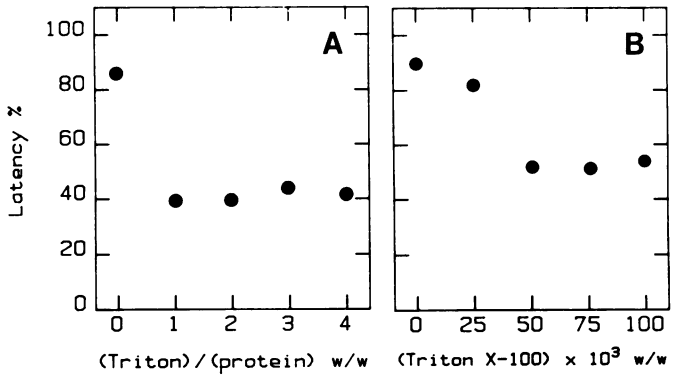

FIG. 1. Effect of various Triton X-100 treatments on the Mg-ATPase latency of plasma membranes purified by phase partition. Basal plasmalemma Mg-ATPase activity (v) was assayed as described in "Materials and Methods." Latency is calculated as $100 \cdot (v_{lysoPC} - v)/v_{lysoPC}$, where v_{lysoPC} is the activity assayed in the presence of 0.1 mM lysoPC. A, Membranes were treated with 0.075% Triton X-100 at various Triton X-100/protein ratios, as described in "Materials and Methods;" B, membranes were treated with 2 mg Triton X-100 per mg protein at various Triton X-100 concentrations.

Membrane Potential of Energized Vesicles. Addition of $MgSO_4$ to KI-washed microsomes caused an increase of the oxonol absorbance in the presence of ATP (Fig. 3, trace a), whereas no response was detected in the absence of ATP (Fig. 3, trace e).

Table II. *Mg-ATPase Latency and Electrogenic H^+-Transport at Successive Steps of Plasma Membrane Purification*

Basal activity and latency of Mg-ATPase were assayed as described in "Materials and Methods." Latency is calculated as $100 \cdot (v_{lysoPC} - v)/v_{lysoPC}$ where v and v_{lysoPC} are the activities in the absence and presence of 0.1 mM lysoPC, respectively. Specifical initial rates of quinacrine quenching and the Mg-ATP-dependent spectral shift of 2 μM oxonol (Ox_b) were measured as described in "Materials and Methods."

	Microsomes	KI-Washed Microsomes	Phase Partition-Purified Plasmalemma	Triton X-100-Treated Plasmalemma
Basal Mg-ATPase activity (μmol · min^{-1} · mg^{-1} protein)	0.10	0.10 ± 0.01	0.11 ± 0.02	0.98 ± 0.09
Latency (%)	69	75	89	51
Initial rate of quinacrine quenching (% · min^{-1} · mg^{-1} protein)	50	50 ± 25	29 ± 13	246 ± 83
Mg-ATP dependent specific spectral shift of oxonol (L · g^{-1})	ND[a]	0.49 ± 0.08	0.40 ± 0.18	2.46 ± 0.89

[a] Not determined.

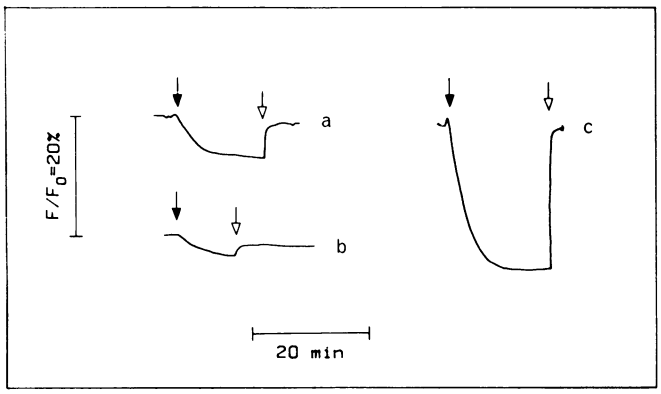

FIG. 2. Mg-ATP-dependent H^+ transport by membrane vesicles at successive steps of plasmalemma purification. Quinacrine quenching (40 μg protein) was measured as described in "Materials and Methods." The reaction was started by addition of 5 mM $MgSO_4$ (closed arrows) and thereafter the pH gradient was dissipated by addition of 10 μM gramicidin (open arrows). Traces are the quenching of quinacrine fluorescence F/F_o, where F_o and F are the fluorescence before and after addition of $MgSO_4$, respectively. a, KI washing; b, phase partitioning; c, Triton X-100 treatment.

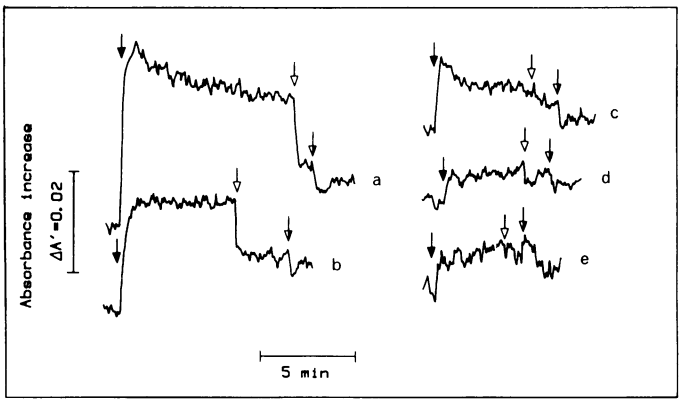

FIG. 3. Effect of various anions on the electrogenic H^+-transport by the Mg-ATPase. KI-washed microsomes (80 μg protein in each case) were incubated for 20 min at 26°C in a medium (pH 6.5) containing 5 mM BTP-ATP (traces a to d), 2.5 μM oxonol and: a, 50 mM BTP-SO_4 and 50 mM K_2SO_4; b, 50 mM BTP-SO_4 and 50 mM K_2SO_4 plus 0.1 μM valinomycin; c, 50 mM BTP-Cl and 100 mM KCl; d, 50 mM BTP-NO_3 and 100 mM KNO_3; e, 50 mM BTP-SO_4 and 50 mM K_2SO_4 in the absence of BTP-ATP. Electrogenic H^+ pumping was initiated by addition of 5 mM $MgSO_4$ (closed arrows) and thereafter membrane potential was dissipated by addition of 10 μM gramicidin in DMSO (open arrows). The effect of the same DMSO aliquot (8 μl) is indicated by half-closed arrows. Traces represent the oxonol absorbance at 622 nm corrected for dilutions due to successive additions, as described in "Materials and Methods."

Addition of gramicidin did not completely reverse the dye response. Furthermore, when the Mg-ATP-dependent absorbance change was small, addition of gramicidin induced a further increase of the dye response (Fig. 4, trace c). This is probably due to interactions between oxonol, membranes, and gramicidin. In the absence of valinomycin, the Mg:ATP-dependent oxonol response was maximum in the presence of SO_4^{2-} (Fig. 3, trace a), strongly depressed when SO_4^{2-} was replaced by Cl^- (Fig. 3, trace c), and was not detected in the presence of NO_3^- (Fig. 3, trace d). This sequence is precisely the one observed for plant membranes' permeability to anions ($SO_4^{2-} << Cl^- < NO_3^-$) (8, 23). When membrane permeability for K^+ was increased by addition of valinomycin, the dye response in SO_4^{2-} was decreased (Fig. 3, trace b), indicating that K^+ short-circuited the pump and thereby decreased its influence on the membrane potential. Thus, the anionic selectivity and valinomycin effect on the dye response are consistent with its membrane potential dependence.

Time-course of absorbance changes of 3.5 μM oxonol by Mg-ATP at successive steps of membrane purification are shown in Figure 4. The dye response was not modified after KI washing of crude microsomes (traces a and b), decreased after phase partition (trace c), and strongly increased after Triton X-100 treatment (trace d), as already observed with quinacrine. The fraction of the dye bound to membranes (Ox_b) can be deduced from the absorption spectrum as described in "Materials and Methods." Titration by oxonol of nonenergized membrane showed that Ox_b increased linearly with concentration of free oxonol (Ox_f) and with protein concentration (data not shown). Mg-ATP-dependent dye binding (ΔOx_b) increased also linearly with Ox_f and protein concentrations (data not shown). Thus, Ox_b and ΔOx_b can be expressed in specific units (mol bound oxonol per mol free oxonol and per g · L^{-1} protein, *i.e.* L · g^{-1}). The variability of the values of Ox_b (*i.e.* in the absence of Mg-ATP) obtained from the different titrations was high, but the mean values of Ox_b at successive steps of purification were not significantly different (2.15 ± 0.47 L · g^{-1} for KI-washed microsomes, 1.76 ± 0.83 L · g^{-1} for phase partition-purified plasmalemma,

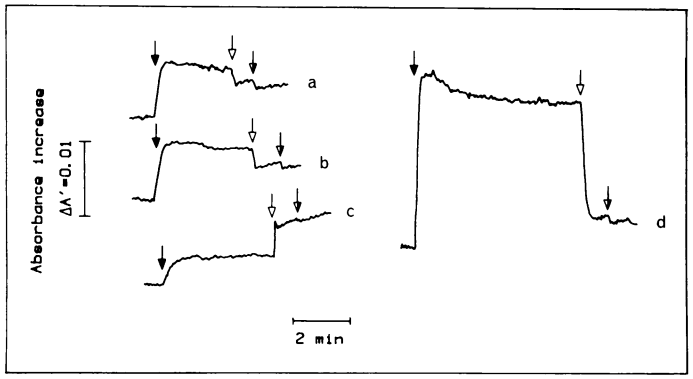

FIG. 4. Electrogenic effect of Mg-ATP dependent H^+-transport at successive steps of membrane purification. Membranes (80 μg protein in each case) were incubated in the presence of 3.5 μM oxonol as described in "Materials and Methods." Electrogenic H^+-transport was initiated by addition of 5 mM $MgSO_4$ (closed arrows), and thereafter membrane potential was dissipated by addition of 10 μM gramicidin in DMSO (open arrows). The effects of the same DMSO aliquot (8 μl) is indicated by half-closed arrows. Traces represent the oxonol absorbance of 622 nm corrected for dilutions due to successive additions, as described in "Materials and Methods." a, Crude microsomes; b, KI-washed microsomes; c, phase partition-purified plasmalemma; d, Triton X-100-treated plasmalemma.

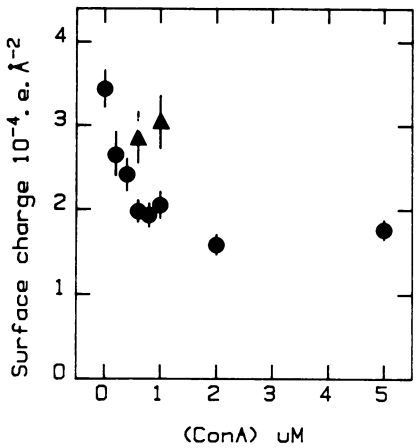

FIG. 5. Electrostatic charge density of plasma membranes as a function of Con A concentration. The microelectrophoretic mobility of 50 vesicles was measured as described in "Materials and Methods." The electrostatic charge density was calculated from the electrophoretic mobility with the help of the Helmholtz-Smoluchowski and Gouy-Chapman relations (see text). (●), In the absence of sugars and (▲), in the presence of 5 mM α-methyl-D-glucopyranoside and 5 mM α-methyl-D-mannoside. The bars are the standard deviations for P = 0.05.

and 2.29 ± 1.56 L · g^{-1} for Triton X-100-treated membranes). The value of ΔOx_b (additional binding after Mg-ATP addition) remained nearly unchanged after phase partition but strongly increased after Triton X-100 treatment (Table II). These results suggest that the modifications of the dye response after vesicle energization at the different steps of plasmalemma purification were truly related to different membrane potentials or proportions of active vesicles and not to different binding properties.

Con A Binding to Phase Partition Purified Plasmalemma, Treated or Not with Triton X-100. The mean electrostatic surface charge density was decreased 50% in the presence of 2 μM Con A (Fig. 5). This effect was due to a specific binding of the lectin to the glucidic cell-coat, as it was prevented by addition of α-methyl-D-mannoside and 1-0-methyl-α-D-glucopyranoside. The dissociation constant of binding sites is 0.4 μM (13). The distribution of the surface charge density in the absence of Con A of 150 vesicles, not treated and treated with Triton X-100, is shown in Figure 6. The mean surface charge densities were 393.10^{-6} ± 98.10^{-6} elementary charge per Å^2 before treatment with Triton X-100 and 305.10^{-6} ± 82.10^{-6} elementary charge per Å^2 after treatment with Triton X-100. In the presence of 1.0 μM Con A, the mean surface charge densities of untreated (n = 300 vesicles) and Triton X-100-treated vesicles (n = 150 vesicles) were 203.10^{-6} ± 79.10^{-6} elementary charge per Å^2 and 209.10^{-6} ± 43.10^{-6} elementary charge per Å^2, respectively. The data were fitted to normal distributions, or linear combination of normal distributions, and Chi-squared tests were used to evaluate the quality of the fits (Table III). In the absence of Con A, it is highly probable, for both Triton X-100-treated and untreated vesicles, that there was a single Gaussian population. In the presence of Con A, the best fit for untreated vesicles was obtained for two mixed populations, each normally distributed with means equal to 327.10^{-6} ± 47.10^{-6} elementary charge per Å^2 (14% of the vesicles) and 179.10^{-6} ± 47.10^{-6} elementary charge per Å^2 (86% of the vesicles). Nevertheless, in the presence of Con A and for Triton X-100-treated vesicles, it is again highly probable there was a single population with a normal distribution.

DISCUSSION

Purity of Plasmalemma after Phase Partition and Triton X-100 Treatment. After phase partitioning of KI-washed microsomes,

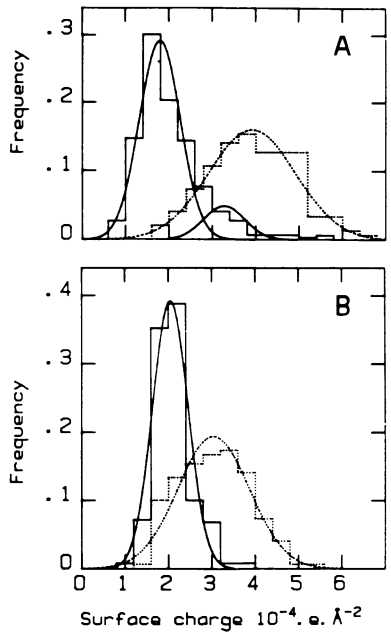

FIG. 6. Effect of Con A on the distribution of the electrostatic charge density of plasmalemma vesicles untreated and treated with Triton X-100. Plasmalemma was purified by phase partitioning. The electrophoretic mobility of vesicles was measured in the absence (discontinuous line) or in the presence (continuous line) of 1.0 μM Con A, as described in "Materials and Methods." The electrostatic charge density was calculated with the help of Helmholtz-Smoluchowski and Gouy-Chapman relations (see text). Bar graphs, observed frequencies of the distribution per interval of 40 10^{-6} e · Å^{-2}; smooth lines, calculated normal distributions (best fit to the observed ones) with means and standard deviations indicated in Table III. A, Untreated plasmalemma (n = 150 vesicles in the absence of Con A, and n = 300 vesicles in its presence); B, Triton X-100-treated plasmalemma (n = 150 vesicles in the absence or in the presence of Con A).

Table III. *Statistical Analysis of the Effect of Con A on the Electrostatic Charge Distribution of Triton X-100-Untreated and Treated Vesicles*

The analysis of the data of Figure 6 was performed with Maximal Likelihood Program (see text). The reported values are those which gave the best fit to the observed data. Observed parameters M, S, N: mean, standard deviation, and number of vesicles, respectively. Theoretical distributions were calculated as normal populations or sum of two normal populations 1 and 2, with parameters M1, S1, N1, and M2, S2, N2. Electrostatic charges are given in $e \cdot Å^{-2} \cdot 10^6$.

Conditions	Observed Parameters			Parameters Used for Fitting						Chi-Squared	
	M	S	N	M1	S1	N1	M2	S2	N2	Obs.	P = 0.05
Untreated, 0 Con A	393	98	150	392	100	150			0	19.8	27.6
Untreated, + Con A	203	79	300	200	69	300			0	76.5	40.1
Untreated, + Con A				327	47	42	179	47	258	24.3	37.7
Treated, 0 Con A	305	82	150	304	82	150			0	20.5	27.6
Treated, + Con A	209	43	150	208	41	150			0	23.7	25.0

30% of the total plasmalemma Mg-ATPase activity (*i.e.* the activity assayed in the presence of lysoPC × protein amount) present in the crude microsomal fraction, and 10% of the proteins were recovered (Table I). The Mg-ATP hydrolysis was almost completely inhibited by vanadate, and the specific activity in the presence of lysoPC (2.4 μmol · min^{-1} · mg^{-1} protein at 38°C) was approximately 3-fold higher than the one in crude microsomes. This value is close to the 3.6-fold enrichment of the plasmalemma Mg-ATP hydrolysis of oat roots, assayed in the presence of Triton X-100, obtained after phase partitioning by Hodges and Mills (14). Phase partitioning of KI-washed microsomes led to the elimination of 80% of tonoplast Mg-ATPase, almost 100% of mitochondrial Mg-ATPase, and 70% of the latent IDPase activity. These results are in agreement with the ones generally obtained for plasmalemma from various tissues and various phase systems (7, 14, 28). Furthermore, approximately 66% of membrane protein was eliminated after Triton X-100 treatment, which completely eliminated the latent IDPase. Nevertheless, approximately 80% of the Mg-ATPase was recovered, and thus its specific activity was increased 2-fold. Such differing solubilizing powers of Triton X-100 on individual membrane components has been already described (19). Finally, the overall purification scheme leads to a 6-fold enrichment of the crude microsomal Mg-ATPase. The specific activity in the presence of lysoPC (4.6 μmol · mg^{-1} protein · min^{-1} at 38°C, Table I), as well as the elimination of contaminants, is the same range as the ones obtained with a similar method by Clement *et al.* (7) for corn shoot plasmalemma (*i.e.* 3.3 μmol · mg^{-1} protein · min^{-1} at 38°C).

Effect of Phase Partition and Triton X-100 Treatment on Mg-ATPase Latency and Electrogenic H^+-Pumping. Contrary to the Mg-ATPase activity observed in the presence of lysoPC, the basal one did not vary after phase partitioning, while the enzyme latency increased from 69 to 89% (Table II). It has been well demonstrated that this latency is due to the permeabilization of right side out vesicles sealed to Mg-ATP, the proportion of which significantly increases after phase partitioning (18). We have previously (13) shown that lysoPC is a suitable permeabilizing agent, which does not directly interact with the enzyme as do Triton X-100 and other surfactants, when used to reveal its latency. Thus, the latency determined with lysoPC gives the true proportion of right side out vesicles. On the other hand, the basal Mg-ATPase activity in 80,000 pellets from corn roots is entirely due to inside out vesicles (and not to open membrane fragments or leaky right side out vesicles) (13). Thus, Mg-ATPase latency at the successive steps of purification indicates that the final percentage of inside out vesicles is three-fold lower than the initial one (from 31% in crude microsomes to 11% after phase partitioning). Finally, the three-fold enrichment in plasmalemma ATPase (demonstrated in the presence of lysoPC, Table I) is counteracted by the three-fold decrease of the proportion of inside out vesicles (Table II). This explains the constancy of the basal specific plasmalemma Mg-ATPase activity of various tissues generally observed after phase partitioning (7, 14, 28).

Triton X-100 treatment resulted in a large increase of the basal Mg-ATPase activity and in a diminution of its latency (from 90 to 50%, Table II). These results indicate an increase in the proportion of catalytic sites freely accessible to Mg-ATP. This increase is likely not due to the permeabilization of right side out vesicles after Triton X-100 treatment, because of the simultaneous increase of specific rate of quinacrine quenching, and Mg-ATP dependent oxonol binding (Table II; Figs. 2 and 4). Furthermore, the initial rate of quinacrine quenching and the oxonol absorbance shift were in the same range when expressed per unit of basal Mg-ATPase activity for treated and untreated purified vesicles (approximately 250% quenching · μmol^{-1} Mg-ATP hydrolyzed and 3 ml · min · μmol^{-1} Mg-ATP hydrolyzed, from Table II). In summary, Triton X-100 treatment, followed by its elimination as described in "Materials and Methods," leads to tightly sealed purified vesicles, as previously reported for nonpurified plasma membranes (13). Triton X-100 elimination, although not checked directly, seems satisfactory, owing to the elimination of the direct inhibiting and permeabilizing effects of this detergent as we have demonstrated previously (13).

Effect of Triton X-100 Treatment on the Accessibility of the Mg-ATPase Catalytic Sites and Con A Binding Sites. The fraction of catalytic sites freely accessible to Mg-ATP increased after Triton X-100 treatment from approximately 10 to 50% (Table II). As previously hypothesized (13), this could be due to the inversion of some right side out vesicles or to their randomization. In the former hypothesis, plasma membranes would keep their asymmetric structure (Mg-ATPase catalytic sites and lectin binding sites exposed on opposite sides of the membrane). In the latter, half of the catalytic and lectin binding sites of randomized vesicles would be exposed outside. Microelectrophoresis experiments show that Con A binding depolarized the membrane surface (Fig. 5). The microelectrophoretic technique used in this study allows the detection of individual particles. Thus, the statistical analysis of the data in Figure 6 allows a direct determination of the proportion of vesicles which bind the lectin (*i.e.* right side out vesicles) or not (*i.e.* inside out vesicles) (13). Approximately 86% of untreated vesicles are capable of Con A binding (Table III), in agreement with the high proportion of right side out vesicles determined from Mg-ATPase latency (89%, Table II). Furthermore, all Triton X-100-treated vesicles were capable of lectin binding and preparations contained only one population of vesicles (Table III). On the other hand, the Mg-ATPase latency indicates that only half of the catalytic sites of

treated vesicles are freely accessible to Mg-ATP (Table II). These data are consistent with a membrane randomization after Triton X-100 treatment, which predicts that half catalytic and lectin binding sites of each vesicle are exposed outside. It has been demonstrated that reintegration of (Na^+, K^+)-ATPase in artificial vesicles leads to a random orientation of the enzyme, half catalytic sites facing inside and half outside in each vesicle (16). It is generally admitted that Triton X-100, around 0.1%, solubilizes membranes, as indicated by the high percentage of protein loss. For instance, Prado *et al.* (22) showed that the percentage of sarcoplasmic reticulum protein recovered in supernatants increased from approximately 30% at 1 mM Triton X-100 (*i.e.* 0.06%, w/w) to 80% at 4 mM, while the major part of the ATPase activity was recovered in the pellets at 1 mM. The 66% protein loss observed at 0.1% Triton X-100 (Table I) agrees with these results. However, the remarkable feature is the presence of membrane vesicles in the pellets, demonstrated by ultrastructural studies on sarcoplasmic reticulum, even when most of protein has been solubilized after Triton X-100 treatment (22). According to these authors, these structures may arise from a reassembly of the solubilized bilayer components.

We have previously hypothesized two mechanisms for explaining the decrease of the Mg-ATPase latency of crude microsomes after Triton X-100 treatment, namely the inversion of right side out vesicles or their randomization (13). Present data are in agreement with the randomization hypothesis. Nevertheless, the previously reported proportion of freely accessible catalytic sites of crude microsomes treated with Triton X-100 was significantly higher (65 ± 6%, four experiments) than the theoretical proportion expected from an ideal randomization (50%). We have repeated these experiments and observed again that Triton X-100 treatment of crude microsomes leads to a significantly higher proportion of accessible catalytic sites (61 ± 2%, six experiments) than the one observed after treatment of phase partition-purified membranes (48 ± 7%, eight experiments). A high proportion of accessible catalytic sites was also observed after purification on sucrose gradient. Although the precise origin of this difference remains unclear, it seems to be related to the method of purification used. The hypothesis of the membrane protein randomization still requires further independent evidence.

In conclusion, we have obtained highly purified corn root plasma membranes after phase partitioning of KI-washed microsomes, and a three-fold enrichment of the Mg-ATPase. Unfortunately, the proportion of inside out vesicles decreased three-fold, and the resulting basal activity of Mg-ATP hydrolysis and electrogenic H^+-transport remain approximately constant in spite of the enzyme enrichment. Indeed, Mg-ATP had access to only 10% of catalytic sites of purified preparations, and thus H^+-transport studies, which necessitate high amounts of protein, are severely impeded. Triton X-100 treatment allows a further two-fold Mg-ATPase enrichment due to non-Mg-ATPase protein loss, while the totality of the plasmalemma Mg-ATPase is recovered as sedimentable vesicles. These vesicles are probably randomized, with half the catalytic sites freely accessible, and remain tightly sealed. The electrogenic H^+ pumping expressed per mg membrane protein strongly increases after Triton X-100 treatment. Nevertheless, its value is not significantly modified when expressed per unit ATPase activity, as has been previously shown for crude plasmalemma fraction (13). Thus, this Triton X-100 treatment seems useful for the studies of plasmalemma transport with highly purified preparations.

Acknowledgments—We thank Suzette Astruc for valuable technical assistance, Dr. G. Ephritikhine for introducing one of us to phase partition method, and Drs. G. Larsson and Ian M. Møller for helpful discussions.

LITERATURE CITED

1. AMES BN 1966 Assay of inorganic phosphate, total phosphate and phosphatases. Methods Enzymol 8: 115–118
2. BANGHAM AD, R FLEMANS, DH HEARD 1958 An apparatus for microelectrophoresis of small particles. Nature 182: 642–644
3. BASHFORD CL, B CHANCE, JC SMITH, T YOSHIDA 1979 The behaviour of oxonol dyes in phospholipid dispersions. Biophys J 25: 63–80
4. BASHFORD CL, B CHANCE, RC PRINCE 1979 Oxonol dyes as monitors of membrane potential. Their behaviour in photosynthetic bacteria. Biochim Biophys Acta 545: 46–57
5. BENNETT AB, RM SPANSWICK 1983 Optical measurements of ΔpH and $\Delta\psi$ in corn root membrane vesicles. Kinetic analysis of Cl^- effects on a proton-translocating ATPase. J Memb Biol 71: 95–107
6. BERCZI A, IM MOLLER 1986 Comparison of the properties of plasmalemma vesicles purified from wheat roots by phase partitioning and by discontinuous sucrose gradient centrifugation. Physiol Plant 68: 59–66
7. CLEMENT JD, JP BLEIN, J RIGAUD, R SCALLA 1986 Characterisation of ATPase from maize shoot plasma membrane prepared by partition in an aqueous polymer two phase system. Physiol Vég 24: 25–35
8. DE MICHELIS MI, MC PUGLIARELLO, F RASI CALDOGNO, L DE VECCHI 1981 Osmotic behaviour and permeability properties of vesicles in microsomal preparation from pea internodes. J Exp Bot 32: 293–302
9. DE MICHELIS MI, RM SPANSWICK 1986 H^+-pumping driven by the vanadate-sensitive ATPase in membrane vesicles from corn roots. Plant Physiol 81: 542–547
10. GALLAGHER SR, RT LEONARD 1982 Effect of vanadate, molybdate and azide on membrane-associated ATPase and soluble phosphatase activities of corn roots. Plant Physiol 70: 1335–1340
11. GIBRAT R, JP GROUZIS, J RIGAUD, C GRIGNON 1985 Electrostatic characteristics of corn root plasmalemma: effect on the Mg-ATPase activity. Biochim Biophys Acta 816: 349–357
12. GREEN JR 1983 The Golgi apparatus. *In* JL Hall, AL Moore, eds, Isolation of Membranes and Organelles from Plant Cells. Academic Press, London, pp 135–152
13. GROUZIS JP, R GIBRAT, J RIGAUD, C GRIGNON 1987 Study of sidedness and tightness to H^+ of corn root plasmalemma vesicles: preparation of a fraction enriched in inside-out vesicles. Biochim Biophys Acta 903: 449–464
14. HODGES TK, D MILLS 1986 Isolation of the plasma membrane. Methods Enzymol 118: 41–54
15. HUNTER RJ 1981 Zeta Potential in Colloid Science. Academic Press, New York
16. KARLISH SJD, WD STEIN 1982 Passive rubidium fluxes mediated by Na-K-ATPase reconstituted into phospholipid vesicles when ATP- and phosphate-free. J Physiol 328: 295–316
17. LARSSON C, P KJELLBOM, S WIDELL, T LUNDBORG 1984 Sidedness of plant plasma membrane vesicles purified by partition in aqueous two-phase systems. FEBS Lett 171: 271–276
18. LARSSON CH 1985 Plasma membranes. *In* HF Linskens, JF Jackson eds, Modern Methods of Plant Analysis, New Series, Vol 1. Springer-Verlag, Berlin, pp 85–104
19. MACDONALD RI 1980 Action of detergent on membranes: differnces between lipid extracted from red cell ghosts and from red cell lipid vesicles by Triton X-100. Biochemistry 19: 1916–1922
20. MACLAUGHLIN S 1977 Electrostatic potential at membrane-solution interfaces. Curr Top Memb Transp 9: 71–143
21. O'NEIL SD, AB BENNETT, RM SPANSWICK 1983 Characterization of a NO_3^- sensitive H^+-ATPase from corn roots. Plant Physiol 72: 837–846
22. PRADO A, JLR ARRONDO, A VILLENA, FM GONI, JM MACARULLA 1980 Membrane-surfactant interactions. The effect of Triton X-100 on sarcoplasmic reticulum vesicles. Biochim Biophys Acta 733: 163–171
23. RASI CALDOGNO F, MC PUGLIARELLO, MI DE MICHELIS 1985 Electrogenic transport of protons driven by the plasma membrane ATPase in membrane vesicles from radish. Plant Physiol 77: 200–205
24. ROSS GJS 1970 The efficient use of function minimization in nonlinear maximum-likelihood estimation. JR Stat Soc C 19: 205–221
25. SCHAFFNER W, C WEISSMAN 1983 A rapid, sensitive, and specific method for the determination of proteins in dilute solution. Anal Biochem 56: 502–514
26. SERRANO R 1985 Plasma Membrane ATPase of Plants and Fungi. CRC Press, Inc., Boca Raton, FL
27. SZE H 1985 H^+-translocating ATPases: advances using membrane vesicles. Annu Rev Plant Physiol 36: 175–208
28. UEMURA M, S YOSHIDA 1983 Isolation and identification of plasma membrane from light-grown winter rye seedlings (*Secale cereale* L. cv Puma). Plant Physiol 73: 586–597